

## Main Manuscript for

# Urban tree deaths from invasive alien forest insects in the United States, 2020-2050.

Emma J. Hudgins<sup>1</sup>, Frank H. Koch<sup>2</sup>, Mark J. Ambrose<sup>3</sup>, Brian Leung<sup>1,4</sup>

<sup>1</sup> Dept. of Biology, McGill University

<sup>2</sup> USDA Forest Service, Southern Research Station

<sup>3</sup> Dept. of Forestry and Environmental Resources, North Carolina State University

<sup>4</sup> School of Environment, McGill University

\*Corresponding author: Emma J. Hudgins.

**Email:** [emma.hudgins@mail.mcgill.ca](mailto:emma.hudgins@mail.mcgill.ca)

**Author Contributions:** EJH and BL conceptualized the study. EJH performed the analyses and created the figures. EJH, BL, FHK and MJA wrote the paper. FHK and MJA provided insect and urban tree expertise and commented on realism of results. MJA manages the urban tree database.

**Competing Interest Statement:** The authors have no competing interests to disclose.

**Classification:** Biological Sciences: Ecology; Social Sciences: Environmental Sciences

**Keywords:** Forest ecology, Economic impact, Scenario modelling, Invasive species

### This PDF file includes:

Main Text  
Figures 1 to 4  
Tables 1 to 1

## 1 Abstract

2 With 70% of the global population in urban centers, the 'greening' of cities is central to future  
3 urban wellbeing and livability. Urban trees can be nature-based solutions for mental and physical  
4 health, climate control, flood prevention and carbon sequestration. These ecosystem services  
5 may be severely curtailed by insect pests, which pose high mortality risks to trees in urban  
6 centers. Until now, the magnitudes and spatial distributions of mortality risks were unknown.  
7 Here, we combine new models of street tree populations in ~30,000 United States (US)  
8 communities, species-specific spread predictions for 57 invasive insect species, and estimates of  
9 tree death due to insect exposure for 48 host tree genera. We estimate that an additional 1.4  
10 million street trees will be killed by insects from 2020 through 2050, costing an annualized  
11 average of US\$ 30M. However, these estimates hide substantial variation: 23% of urban centers  
12 will experience 95% of all insect-induced mortality, and 90% of all mortality will be due to emerald  
13 ash borer (*Agrilus planipennis*, EAB). We define an EAB high-impact zone spanning 902,500km<sup>2</sup>,  
14 largely within the Midwest and Northeast, within which we predict the death of 98.8% of all ash  
15 trees. "Mortality hotspot cities" facing costs of up to US\$ 13.0 million each include Milwaukee, WI,  
16 Chicago, IL, and New York, NY. We identify Asian wood borers of maple and oak trees as posing  
17 the highest future risk to US urban trees, where a new establishment could cost US\$ 4.9B over  
18 the same time frame.

## 19 Significance Statement

20  
21 US urbanization levels are already at 82% and are growing, making losses of ecosystem services  
22 due to urban tree mortality a matter of concern for the majority of its population. To plan effective  
23 mitigation, managers need to know which tree species in which parts of the country will be at  
24 greatest risk, as well as the highest-risk insects. We provide the first country-wide, spatial  
25 forecast of urban tree mortality due to invasive insect pests, including forecasts for each host tree  
26 and each insect species in each US community. This framework identifies dominant pest insects  
27 and spatial hotspots of high impact. Further, these findings produce a list of biotic and  
28 spatiotemporal risk factors for future high-impact US urban forest insect pests.

## 30 Main Text

### 32 Introduction

33  
34 Previous analyses suggest that impacts associated with urban trees are likely to comprise the  
35 dominant share of economic damages caused by invasive alien forest insects (IAFIs) in the  
36 United States (US) [1]. Urban tree populations include highly susceptible species like ash  
37 (*Fraxinus spp.*) that are being decimated by emerald ash borer (EAB, *Agrilus planipennis*) [2]. To  
38 eliminate the potential for injury or property damage due to dead trees, infested urban trees must  
39 be treated or removed [3]. Moreover, the importance of urban forests is only expected to grow.  
40 While urbanization is already very high in the US (82% in 2018), it has not yet reached saturation  
41 (World Bank, <http://data.worldbank.org>, UN DESA, <http://population.un.org>). At the same time,  
42 there has been a push for urban 'greening' (i.e., increasing urban forest canopy). Urban trees  
43 perform many important ecosystem services, including lowering cooling costs [4], buffering  
44 against flooding, increasing air quality, carbon sequestration, improving citizens' mental and  
45 physical health outcomes, and creating important habitat [5,6]. The high tree mortality risk posed  
46 by IAFIs can greatly diminish these myriad benefits.

47 While IAFI life histories differ, they are known to be transported long distances by  
48 humans [7], potentially with similar drivers across entire dispersal pathways [8]. Thus, the  
49 creation of a pathway-level damage estimate can provide insight into the benefit of limiting future  
50 spread via these pathways (e.g. through quarantines, highway checkpoints to limit firewood

51 movement). Past estimates of IAFI damage have been important in providing support for  
52 phytosanitary measures such as ISPM15 [10], a wood packing material treatment protocol,  
53 whose adoption is growing worldwide [11]. A previous pathway-level estimate for the cumulative  
54 cost of all US IAFIs was performed a decade ago and had substantial data limitations [1]. Since  
55 then, contemporary advances allow direct estimates of spread for every IAFI species as well as  
56 host prevalence and IAFI-induced mortality for every tree species in every community across the  
57 United States. This allows not only the estimation of country-wide IAFI damages, but also IAFI  
58 and host-specific damages and their spatial distribution. Further, we can examine the impact of  
59 tree mortality dynamics on cost dynamics, and derive better risk assessments of not-yet  
60 established pests, based their functional traits and host distributions.

61 In this paper, we synthesized four subcomponent models of IAFI invasions: 1) a model of  
62 57 IAFI species' spread, 2) a model for the distribution of all urban street tree host genera across  
63 all US communities, 3) a model of host mortality in response to IAFI-specific infestation for all  
64 urban host tree species, and 4) the cost of removing and replacing dead trees, to provide the best  
65 current estimate of the damage to street trees, including explicit estimates for all known IAFIs  
66 across all major insect guilds (Fig. S1-S2).

67

## 68 Results

69

### 70 Urban tree pest exposure

71 Total tree abundance models were predictive with some outliers (Appendix S1, Fig. S4, small  
72 trees:  $R^2 = 0.78$ , medium trees:  $R^2 = 0.58$  large trees:  $R^2 = 0.42$ ). Removing the outliers changed  
73 the  $R^2$  to 0.76 for small trees, 0.76 for medium trees, and 0.58 for large trees. Our genus-level  
74 abundance models were strong but became slightly weaker for rare genus - size class  
75 combinations (Fig. 1, overall  $R^2$  for all genera of small trees:  $R^2 = 0.93$ , medium trees:  $R^2 = 0.93$ ,  
76 large trees:  $R^2 = 0.92$ ). While relationships were variable across genera, the genera that were fit  
77 most poorly did not make up a large proportion of predicted trees, and none were below  $R^2 = 0.25$   
78 (Fig. S5).

79 We tested four model types (global BRT, global GAM, customized BRT, or customized  
80 GAM) to fit 1) genus-level tree presence/absence and 2) genus-level abundance models (Fig.  
81 S1). The optimal genus-level fitting approach differed across genera depending on diameter  
82 class, prevalence of genera, and whether presence/absence or tree abundance was the  
83 response variable (Table S2). Generally, rarer genera were better fit by global BRT and GAM  
84 models, which utilized information from all other species while common species were better fit by  
85 customized models (Fig. S6). According to our models, while subject to regional variation, the  
86 population of street trees is mostly made up of maple (*Acer*) and oak (*Quercus*), with substantial  
87 ash (*Fraxinus*, Fig. S7).

88 We analyzed street trees separately from residential and community trees. Predicted  
89 street tree exposure (measured as the number of predicted susceptible trees in Fig. 2a \* IAFI  
90 relative propagule pressure in Fig. 2b, [8]) across all tree types from 2020 to 2050 was generally  
91 high in the eastern US, and only sporadically high across the western US (Fig. 2c). Predicted  
92 street tree exposure was highest among maples (*Acer* spp., 25.6M predicted exposed trees),  
93 oaks (*Quercus* spp., 5.9M), and pines (*Pinus* spp. 3.4M). The greatest number of trees were  
94 predicted to become exposed to Jose scale (*Quadraspidiotus perniciosus*, 7.3M), Japanese  
95 beetle (*Popillia japonica*, 6.7M), calico scale (*Eulecanium cerasorum*, 6.4M), San. Among  
96 residential and community trees, exposure was greatest among maples, oaks, and *Prunus* spp.  
97 (1.7B, 1.1B, 707M, respectively), and the most frequently predicted IAFI encounters were with the  
98 same three species (Japanese beetle, San Jose scale, and calico scale).

99

### 100 Host tree mortality

101 The best-fitting mortality model indicated that most IAFIs fall in the low severity groups. Within all  
102 severity groups, the majority of IAFIs were at the low end of severity (Fig. 3, full results in  
103 Appendix S2). We define the term 'mortality debt' as the time period between an IAFI initiating  
104 damage within a community and reaching its estimated asymptotic host mortality within that

105 community (see *Methods*). In our most likely mortality debt scenario (i.e., 10-year scenario for  
106 borers, 50-year scenario for defoliators, 100-year scenario for sap feeders), we estimated a  
107 mortality level of 0.7-2.5% beyond expected natural mortality of street trees by 2050, where our  
108 most likely scenario fell on the higher end of this range (Table 1). Predicted street tree death  
109 varied by a factor of four based on the mortality debt scenario, with longer debts leading to lower  
110 total mortality between now and 2050 (Table 1). This was because in longer mortality debt  
111 scenarios, trees experience mortality in the years 2020-2050 from IAFIs that initially established  
112 in their communities in 2000 (50yr debt) or 1950 (100yr), but our highest impact IAFI (EAB) can  
113 only begin to cause mortality after 2002 in any scenario. Sensitivity was driven largely by wood  
114 boring species, as demonstrated by the sensitivity of mortality estimates to their mortality debt  
115 scenarios (“Vary Borers” row, Table 1). We also found that longer mortality debts lead to a  
116 smoother cost curve, or costs that do not vary much due to more consistent host mortality rates  
117 (Fig. 4).

118 Spatially, future damages will be primarily borne in the Northeast and Midwest, driven by  
119 EAB spread (Fig. 2d). We predict that EAB will reach asymptotic mortality in 6747 new cities,  
120 which means that 98.98% of its preferred *Fraxinus* spp. hosts will die. Thus, the mortality is  
121 predicted to be concentrated in a 902,500km<sup>2</sup> zone encompassing many major Midwestern and  
122 Northeastern cities (Fig. S10). This mortality is also predicted to result in a 98.8% loss of all ash  
123 street trees within this zone. Over 230,000 ash street trees are predicted to have died before  
124 2020, and there are a further 69 cities where EAB is predicted to reach asymptotic mortality within  
125 10 years of 2050 (i.e., 98.8% ash mortality by 2060). Due to the restricted range of forest ash  
126 relative to urban ash, we predict that 68% of ash trees and 76% of communities containing street  
127 ash will remain unexposed to EAB in 2060. Furthermore, at-risk ash trees are unequally  
128 distributed. We projected the highest risk close to the leading edge of present-day EAB  
129 distributions, particularly in areas predicted to have high ash densities. The top “mortality hotspot  
130 cities”, where projected added mortality is in the range of 5,000-25,000 street trees, include  
131 Milwaukee, WI, the Chicago Area (Chicago/Aurora/Naperville/Arlington Heights, IL), Cleveland,  
132 OH, and Indianapolis, IN (Fig. 2d). Cities predicted to have high mortality outside of the Midwest  
133 include New York, NY, Philadelphia, PA, and Seattle, WA – communities with high numbers of  
134 street trees and high human population densities, which attract EAB propagules within our spread  
135 model. The states most impacted by street tree mortality match these patterns, where the highest  
136 mortality is predicted for Illinois, New York, and Wisconsin.

137

### 138 Cost estimates

139 We estimated annualized street tree costs across all guilds to be between US\$29-33M per year in  
140 our most likely scenario (mean = \$30M, Table 1, Fig. S11). Roughly 90% of all costs across the  
141 entire US were due to EAB-induced *Fraxinus* spp. mortality. The total cost associated with street  
142 tree mortality in the top ten hotspot cities was estimated at \$50M from 2020 to 2050, with \$13M in  
143 Milwaukee, WI alone.

144 The ranking of feeding guild severity was relatively robust across mortality debt  
145 scenarios, in spite of the potential for differences due to the interaction of IAFI-specific spread  
146 and mortality debt dynamics. Costs were higher for longer mortality debt scenarios for borers,  
147 peaked at intermediate debt for defoliators, and peaked at the longest debt for sap feeders.  
148 These patterns were due to the relative rates of historical and contemporary range expansion of  
149 more impactful IAFIs (i.e. high impact borers have more rapid recent range expansion, while  
150 contemporary high impact defoliator expansion is slow compared to 50 years ago). Borers were  
151 predicted to be the most damaging feeding guild (\$8M-28M mean annualized street tree  
152 damages across scenarios), and EAB was consistently the top threat. Defoliators were predicted  
153 to be the second most damaging feeding guild in the next 30 years (means = \$0.8M-\$1.4M), in  
154 spite of more widespread hosts than wood borers, due to lower asymptotic mortality levels.  
155 Defoliators had a 1-2 order of magnitude lower cost than wood-boring species, but again showed  
156 consistency in which species were the top threats within the guild. Consistent with previous work  
157 in [1], European gypsy moth had the highest cost of all defoliators, followed by Japanese beetle  
158 and cherry bark tortrix (*Enarmonia formosana*). The sap-feeding group accrued the lowest costs

159 in the next 30 years due to their lower asymptotic mortality and rarer street tree hosts (mean =  
160 \$0.2M-1.1M). Hemlock woolly adelgid (*Adelges tsugae*) was the highest impact sap feeder,  
161 followed by oystershell and elongate hemlock scale insects (*Lepidosaphes ulmi*, *Fiorinia externa*).  
162 Total costs were only notably sensitive to borer mortality debt scenario misspecification (Table 1),  
163 which is promising, given our certainty of the shorter scenario for EAB.

#### 164 165 Potential impacts to non-street trees

166 Mean added mortality (i.e. above background rates) for residential and non-residential community  
167 trees in the most likely scenario was 1.0% (13.3M residential and 72.1M non-residential trees,  
168 Table S10). While recognizing that non-street tree management will likely be more variable, to  
169 provide a rough estimate, we assumed that non-street trees would be managed in the same way  
170 as street trees (i.e. removal and replacement of dead trees). In this scenario, added mortality  
171 would incur an estimated annualized cost of \$1.5B for non-residential trees and \$356M for  
172 residential trees. Further, a disproportional amount of the total damages (91% of the mortality to  
173 residential non-residential community trees) is expected to be felt in the aforementioned hotspot  
174 zone, with 12.1 million residential and 65.9 million non-residential community trees expected to  
175 be killed. Given the relatively limited data, and the difference in potential management behaviour  
176 for these trees, we caution against overinterpretation of these results.

#### 177 178 Novel IAFI risk forecast

179 Our framework allowed us to identify the factors leading to the greatest impacts for IAFIs already  
180 known to have established in the United States. We were able to identify the most common urban  
181 host trees, the sites facing the greatest future IAFI propagule pressure, and the IAFI-host  
182 combinations with the greatest mortality. However, this approach can also be synthesized with  
183 IAFI entry scenarios to understand potential impacts of novel invasive IAFIs. To illustrate the  
184 utility of this framework predictively, we have provided a checklist of risk factors in Table S11 and  
185 future spread simulations in Table S12 and Fig. S12. We show that entry via a southern port (e.g.  
186 the Port of South Louisiana) would lead to the greatest number of exposed trees. Further, an  
187 EAB-like borer of oak and maple trees could kill 6.1 million street trees and cost \$4.9B over the  
188 next 30 years.

#### 189 190 191 **Discussion**

192  
193 While previous analyses have indicated that urban trees are associated with the largest share of  
194 economic damages due to IAFIs [1,13,14], until recently, data did not exist on the urban  
195 distribution of host trees [15], the spread of IAFIs [8], nor the mortality risk for hosts due to  
196 different IAFIs [16]. With these new models, it is now possible to forecast where and when IAFIs  
197 will have the most damages across the US. Our analysis suggests an overall added mortality of  
198 between 2.1-2.5% of all street trees, amounting to \$US 30M per year in management costs.  
199 However, the most interesting and potentially useful element was our ability to forecast hotspots  
200 of future forest IAFI damages, including a 902,500km<sup>2</sup> region that we expect to experience 95.7%  
201 of all mortality, in large part due to a 98.8% loss of its ash street trees due to EAB. This type of  
202 forecasting has been highlighted as a crucial step in prioritizing management funds [17]. These  
203 data can be used by municipal pest managers to anticipate future costs, and may help motivate  
204 improved spread control programs that aim to identify the potential source counties of future  
205 invasions and mitigate the worst anticipated impacts (complete forecast available at  
206 <http://github.com/emmajhudgins/USStreedamage>).

207 Beyond present IAFI risks, our integrated model can also act as a risk assessment tool  
208 for street tree mortality caused by novel IAFIs (Table S11-S12, Fig. S12). While ash trees are  
209 assured to be dramatically affected by EAB over the next few decades, our models suggest oak  
210 and maple to be the most common street tree genera nationwide. Further, while ash species are  
211 being substituted for less susceptible tree species, maples and oaks continue to be widely  
212 planted within our street tree inventories. Therefore, IAFIs with host species spanning these

213 genera should be of heightened concern. Secondly, the timescale and magnitude of the impacts  
214 of wood borers (see also [1]) make them the highest risk to street trees. We integrated these two  
215 pieces of information with information on major ports of entry within the US (American Association  
216 of Port Authorities 2015, <http://aapa.com/>), as well as our general model of IAFI spread [8], to  
217 forecast the extent of exposed maple and oak street trees from 2020-2050 (Fig. S12, Table S12).  
218 Our analyses show that entry via a southern port would lead to the greatest number of exposed  
219 trees. Further, larger trade volumes between the US and Asia compared to other regions [18]  
220 suggest Asian natives will be the most likely future established IAFIs. One potential candidate  
221 species fitting these criteria is citrus longhorned beetle, which is an Asian wood borer thought to  
222 have many potential host species within the United States, including ash, maple and oak [19].  
223 The lack of more thorough regulation of live plant imports and strict implementation of current  
224 wood treatment protocols such as ISPM15 [20] increase the susceptibility of the US to invasion  
225 and subsequent spread of this species and other potentially high-risk borers.

226 Our impact estimates vary substantially based on dynamics of host mortality following  
227 initial IAFI invasion, especially because of variability in the duration and functional form of  
228 mortality debt. Luckily, the guild (borers) and species (EAB) whose impact on total community  
229 costs are most sensitive to correct specification of the mortality debt dynamics are the ones for  
230 which we are most confident. Several publications have demonstrated near-complete decimation  
231 of ash stands in the decade following EAB infestation [2,21,22]. Furthermore, since total tree  
232 mortality is asymptotically equivalent across all mortality debt regimes, if other feeding guilds  
233 possessed 10-year mortality debt regimes, we should have been able to detect a rapid die-off of  
234 their hosts as they spread, similarly to what we found for EAB (albeit scaled by their maximum  
235 mortality rates). This is not the case in the literature [22].

236 With our integrated model, we also estimated economic damages, which updates the  
237 decade old Aukema et al. [1] using recent advances [13,14]. Surprisingly, the previous cost  
238 estimates were not that different at the country scale. The previous cost estimate separated  
239 urban trees into residential and non-residential types (grouping street trees in the latter). We  
240 estimate annualized costs for non-residential trees to be somewhat lower than those in [1] (\$1.3B  
241 versus \$2.0B in total “Local Government expenditures”). This lower estimate is likely because of a  
242 lower rate of predicted *Fraxinus* exposure to EAB (i.e., lower predicted ash abundance in areas of  
243 predicted EAB spread) in non-residential areas. Interestingly, our estimate of residential tree  
244 costs is roughly one third that in [1] (\$303M vs \$1.1B in total “Household Expenditures”), again  
245 likely due to a (more extreme) overestimate in the nationwide prevalence of residential ash trees  
246 in the previous publication.

247 Additionally, we predict that 75% of communities containing ash trees and 68% of all  
248 street ash will remain untouched by EAB by 2060 because of the lack of forest ash beyond our  
249 forecasted invasion extent (i.e., affecting exposure). However, in some EAB infested  
250 communities, it is important to note that our street tree distributional model may overestimate the  
251 tree mortality projected, due to the role of preventative cutting prior to EAB arrival, which occurred  
252 in many cities across IN, IL, MI, and WI. Preventative cutting would have led to the payment of  
253 tree removal costs prior to our estimation window. This is particularly likely to have inflated the  
254 2020-2050 costs to communities with large street tree budgets in regions where EAB was  
255 predicted to invade in the years 2010-2020 (therefore initiating mortality 2020-2030).

256 Spatially, our results show clear patterning of high threat in the eastern and central US,  
257 and lower threat in the western US. This pattern is consistent with previous findings [20], and can  
258 be explained by the high impacts of EAB, European gypsy moth, and hemlock woolly adelgid,  
259 whose distributions are projected to concentrate further east in the short term. However, some of  
260 the highest-impact non-native pathogens have emerged in the western US, and were not  
261 captured in this analysis [23,24]. Western regions could also see high future risks due to the  
262 polyphagous shot hole borer (*Euwallacea whitfordiodendrus*), and its insect-disease complex with  
263 fusarium fungus (*Fusarium spp.*) [25]. This complex has already established in California and has  
264 maple and oak trees among its many hosts.

265 While the substantial advances that emerged recently allowed us to develop a more fully  
266 integrated model, we also identified data deficiencies which require additional research. A relative

267 quantification of additional sources of uncertainty is provided in Appendix S3. This cost estimate  
268 is arguably a lower bound, since it only examines the cutting of dead trees. The analysis also fails  
269 to account for preventative management, to fully examine non-street tree management, and to  
270 assess the impacts of IAFIs that have not yet established in the United States. Furthermore, our  
271 analysis assumes a complete identification of 'high impact IAFIs'. Some presently established US  
272 may not yet have been identified as 'high impact', either due to lags in their impact, and/or lags  
273 the detection of this impact [26], but may achieve the same level of recognition as those in [1]  
274 before 2050.

275

### 276 Conclusion

277 We have shown that the suite of known IAFIs have the potential to kill roughly a hundred million  
278 additional urban trees in the US in the next 30 years. While these numbers themselves are  
279 striking, reporting only a country-level impact estimate without IAFI species, tree, and community-  
280 level resolution does little to inform management prioritizations. Here, we were able to identify  
281 specific urban centers, IAFI species, and host tree genera associated with the vast majority of  
282 these impacts. We predict that 90% of all street tree mortality within the next 30 years will be  
283 EAB-induced ash mortality, and that ~95% of all street tree mortality will be concentrated in less  
284 than 25% of all communities. These estimates illustrate the gravity of IAFI infestations for  
285 communities in the path of high impact invaders that are rich in susceptible hosts. Further, we  
286 were able to use this framework to identify a checklist of biotic and spatiotemporal risk factors for  
287 future high-impact street tree IAFIs.

288

### 289 **Materials and Methods**

290

291 We synthesized four subcomponent models of IAFI invasions: 1) a model of 57 IAFI species'  
292 spread, 2) a model for the distribution of all urban street tree host genera across all US  
293 communities, 3) a model of host mortality in response to IAFI-specific infestation for all urban host  
294 tree species, and 4) a simple model of the human management response to dead host trees, to  
295 provide the best current estimate of the damage to street trees (see conceptual diagram, Fig. S1).

296

#### 297 IAFI dispersal forecasts

298 We modelled spread using the Semi-Generalized Dispersal Kernel (SDK, [8]). This is a spatially  
299 explicit, negative exponential dispersal kernel model that can account for additional spatial  
300 predictors in source and recipient sites. The SDK builds from the Generalized Dispersal Kernel  
301 (GDK, [8]) as a starting point, using human population density, forested land area and tree  
302 density in source and destination sites as moderators of spread. The SDK combines up to three  
303 species-specific corrections for each species to maximize predictive ability: 1) a species-specific  
304 intercept term, 2) information on an IAFI's likely initial invasion location, and 3) niche-related  
305 limitations when evidenced in the literature. The SDK was applied to all 57 IAFIs believed to  
306 cause some damage from [1], and projected from 2020 to 2050 (Fig. S2).

307

#### 308 Street tree models

309 Our fitting set consisted of 653 street tree databases for US communities where street tree  
310 inventory data had been collected (Fig. S3, [14]). In two communities (Tinley Park and, IL and  
311 Fort Wayne, IN), preventative cutting for EAB was conducted prior to the most recent inventory  
312 and was therefore accounted for within our dataset. We modelled the abundance and diameter at  
313 breast height (DBH) for trees within each genus, as treatment costs are dependent on number  
314 and diameter of trees [1]. We split trees into three diameter classes (small = 0-30cm, medium =  
315 31-60cm, large >60cm). We first fit models for the total tree abundance of all species by diameter  
316 class, and then used these total tree models to help predict genus-specific tree abundance within  
317 each diameter class. Street tree inventory data are not always reliably reported to the species  
318 level across municipalities, and some species are so rare in street tree inventories that it would  
319 have been very difficult to develop robust species-level models, so we limited our examination to  
320 the genus level. Since IAFIs may not be equally impactful to all host tree species in a genus, we

321 had to estimate the genus-level severity of each IAFI species for each IAFI-host combination. We  
 322 did so by estimating the species-level breakdown of each genus based on their average relative  
 323 proportions across our 653 inventoried communities, and assuming this distribution was  
 324 representative in other projected communities.

325 We modelled the total abundance of street trees in a community using boosted  
 326 regression trees (BRT, *gbm.step* within R package *dismo*, [27]) relating the logarithmically-scaled  
 327 total tree abundance within a diameter class to community-specific predictors, employing  
 328 environmental variables from WORLDCLIM [28] and community characteristics used in [13], and  
 329 sourced largely from the National Land Cover Database (NLCD,[29]), the US Census and the  
 330 American Community Survey (<https://www.census.gov/data.html>, Table S1). We hypothesized  
 331 that the age and wealth of a community would influence the types and sizes of trees planted  
 332 there. In our model, median home value and mean year of construction (at the block-group level)  
 333 as well as median household income (at the county level) were used as proxies of the age of the  
 334 urban tree community and the community budget for street trees. We also tested the use of  
 335 Poisson GAM models, but high levels of concurrency (the GAM equivalent of multicollinearity, [30])  
 336 amongst predictors and lower predictive performance indicated Poisson GAMs were an inferior  
 337 modelling structure for estimating total abundance.

338 Next, we estimated the abundance of street trees within each genus, using the same  
 339 climatic and demographic factors as the total tree abundance model as well as the total tree  
 340 abundance model output as predictors (Fig. S1). We considered two approaches: 1) Zero-inflated  
 341 Poisson GAMs, or 2) a two-step BRT approach. For BRT, we modeled tree presence/absence,  
 342 followed by tree abundance given presence (using logarithmically-scaled tree abundance and  
 343 back-transforming when predicting), and then combined the two models. The number of trees of  
 344 genus  $i$  in size class  $j$  at a particular site  $k$  was:

$$345 \quad trees_{i,j,k} = c_{i,j,k} * pred_{exist,i,j,k} * pred_{number,i,j,k} \quad (1)$$

$$346 \quad c_{i,j,k} = \frac{1}{\sum_k(pred_{exist,i,j,k} * pred_{number,i,j,k}) / \sum_k obs_{number,i,j,k}} \quad (2)$$

347 This process is similar to a zero-inflated Poisson (ziP) model [31] but does not link the  
 348 parameters of the binary and continuous components of the model, instead fitting them  
 349 separately. Because our BRT approach was built from two independent parts, we needed to add  
 350 a rescaling step so that the output summed to the observed counts (eqn. 2), as occurs for ziP  
 351 models by default [31]. We removed all highly correlated variables ( $r > 0.8$ ) prior to fitting, and  
 352 refit GAMs until maximum estimated worst-case concurrency using three-knot smoother functions  
 353 was below 0.8 (*concurrency* function within *mgcv*,[32]).

354 We compared BRT and GAM models that were fit to all genera simultaneously (general  
 355 BRT/GAM models using genus-specific intercept terms) with models that were fit to each genus  
 356 separately (customized BRT/GAM models) (Fig. S1). Predictive power could be higher when  
 357 modelling all genera together if the genera respond similarly to predictors, while power could be  
 358 higher for individually fitted genera where environmental and community characteristic  
 359 relationships are idiosyncratic and where the sample is sufficiently large.

360 We chose the model that produced the strongest relationship for each genus using  $R^2$   
 361 values that were relative to the 1:1 line (i.e. a normalized mean squared error,  $R^2_{MSE}$ ).  $R^2_{MSE}$  more  
 362 correctly measures deviations between observations ( $y$ ) and predictions ( $\hat{y}$ ) than conventional  $R^2$ .

$$363 \quad R^2_{MSE} = 1 - \frac{\sum(y-\hat{y})^2}{\sum(y-\bar{y})^2} \quad (3)$$

364 We removed New York, NY from the fitting set as it was likely to be a high leverage observation  
 365 and could have significantly changed the resulting models due to it possessing a markedly  
 366 different street tree genus composition from all other communities. Both the GAM and BRT  
 367 models were fitted using their built-in cross-validation algorithms for parameter estimation, and  
 368 can therefore tolerate occasional outliers with minimal effect on their parameter estimates (though  
 369 we have less evidence that other outliers would have changed model parameters for cities other  
 370 than New York, NY). Given the higher data requirements of GAMs (i.e. all parameters must be fit  
 371 simultaneously, rather than BRT, which can fit subsets of predictors to each tree, [33]), genus-  
 372 specific GAMs were not considered when data were insufficient (i.e., when only a few cities



373 contained that genus). For each genus, we used the best-fitting model to predict urban tree  
374 distributions throughout the contiguous US. We used the observed number of trees rather than  
375 model predictions in cities where these data were available. Alaska and Hawaii were removed to  
376 match the spatial extent of IAFI spread predictions, and because urban tree genus composition is  
377 likely quite different in these areas compared to the contiguous US.

378 We synthesized the previous two modelling steps, intersecting IAFI spread forecasts with  
379 predicted tree distributions (using observed tree data where available), to create forecasts of tree  
380 exposure, which we define as the sum of predicted density of each IAFI species, multiplied by  
381 their predicted host tree abundance in each community.

382

### 383 Host mortality model

384 We examined the impacts of the three major feeding guilds of IAFIs [34]: Foliage feeders included  
385 insects that feed on leaf or needle tissue. Sap feeders included all species that consume sap,  
386 including scale insects and gall-forming species. Borers included species that feed on phloem,  
387 cambium, or xylem. Across insect guilds, the logic from [1] appeared to hold: most species were  
388 innocuous, but a small number caused high mortality (Table S7). In contrast, while several  
389 invasive pathogens were mentioned in [14], pathogens are only reliably reported when they  
390 produce noticeable (i.e. intermediate) impacts [1]. To avoid mischaracterizing their impacts, we  
391 removed pathogens from the remainder of our analysis.

392 We ranked the severity of a given IAFI infestation on a particular host using a scale  
393 based on observed long-term percent mortality (defined in [14], Table S7). We added two  
394 additional categories to this scale to represent IAFI species missing from their database that are  
395 still considered pests on a particular host in [1]. The lowest-impact IAFI-host combinations were  
396 those featuring IAFIs reported as 'low impact' in [1]. These accounted for most known  
397 combinations. The second lowest category featured 'intermediate impact' IAFI species from [1]  
398 that did not appear as threats to a given known host in [14]. We assumed that, were these  
399 species quantified by [14], their associated severities would be lower than the lowest category  
400 within the authors' ranking scheme. All other IAFI-host combinations were assigned to the same  
401 categories as in [14]. IAFI frequency within severity categories was normalized across the sum of  
402 their known hosts so that each IAFI had equal impact on the frequency distribution (i.e.,  
403 frequency summed to 1 for each IAFI). For instance, if an IAFI had 3 hosts, and had severities of  
404 3, 5, and 9 on each host, we would give them a frequency of 1/3 under each bin. We fit a Beta  
405 distribution to the frequency distribution of IAFIs in each of these categories using Stan [35], a  
406 program and language for efficient Bayesian estimation. We chose to fit a Beta distribution  
407 because proportional mortality ranged between 0 and 1. Additionally, we fit the upper limit of the  
408 two lowest mortality categories and the lower limit of the highest category, as these categories did  
409 not have quantified bounds, but could be ranked relative to others. We used the posterior mean  
410 as the expected mortality for an IAFI in each severity category, rather than the simple midpoint of  
411 the range of each category.

412 We define the term 'mortality debt' as the time period between an IAFI initiating damage  
413 within a community and reaching its estimated asymptotic host mortality within that community.  
414 While we had estimates of the asymptotic proportional mortality of host trees [14], we had no  
415 information on the rate by which trees reach this plateau. Previous estimates have ranged from 5  
416 to 100 years [1,36], so we analyzed three scenarios within this range (10, 50, 100 years). To  
417 account for what is currently known about the mortality dynamics of IAFIs within each of the  
418 feeding guilds, we also examined scenarios based on our most likely scenario of the duration of  
419 mortality debt across IAFI feeding guilds. EAB is estimated to kill the majority of its susceptible  
420 hosts in the first decade following infestation [19], while maximum mortality is estimated to take  
421 closer to 100 years for hemlock woolly adelgid [1], so we used the 10 and 100-year scenarios for  
422 borers and sap-feeders, respectively. A recent publication examining mortality rates in forested  
423 areas suggested that European gypsy moth has a mortality rate intermediate between borers and  
424 sap-feeders, so we set defoliators at 50-years [20]. Once an IAFI was predicted to infest an area,  
425 we imposed a 10-year initial lag phase between IAFI arrival at a site and the initial onset of  
426 damage [37,38] and then began increasing the host mortality following our mortality debt scenario

427 to the asymptotic level (defined by the host mortality model). For simplicity, we assumed  
428 mortality increased by a constant fraction over time until reaching its maximum and levelling off.  
429 For example, in the 50-year mortality debt scenario, if an IAFI's maximum host mortality was  
430 defined as 90%, mortality would increase by 9% at each 5-year timestep for 10 timesteps until  
431 90% mortality had been reached.

432 The joint impact of maximum mortality and mortality debt is best illustrated by a series of  
433 examples. Estimates of street tree natural mortality range around 2.4-2.6% per year [12]. Within a  
434 30-year window, this would amount to roughly 53% natural street tree mortality. Our model  
435 assumes that if IAFI enters site at the beginning of this window (2020), it first undergoes a 10-  
436 year time lag, and can then cause mortality in the final 20 years. The maximum level of mortality  
437 induced by a borer (EAB on several *Fraxinus* spp., Category H = 98.98%), would result in 98.98%  
438 additional mortality (mortality of remaining the trees that survived natural mortality) at the end of a  
439 30-year window. This level of mortality would be clearly detectable above natural street tree  
440 mortality. Hemlock woolly adelgid has a similar maximum mortality to EAB (Category H on *Tsuga*  
441 spp.), but we have assumed that sap-feeder mortality takes 100 years to reach asymptotic levels.  
442 As such, by the end of a 30-year window, only  $(98.98\%/100) \times 20$  years = 19.80% of additional  
443 host trees would be killed. While defoliators have shorter mortality debts, they tend to cause lower  
444 mortality, making their impacts the least detectable above background mortality. For defoliators,  
445 the IAFI with the greatest damage on any host is the larch casebearer, (*Coleophora laricella* on  
446 *Larix laricina*, category E = 16.46%). Given a 50-year mortality debt for defoliators, the maximum  
447 mortality above background rates by 2050 is  $(16.46\% / 50) \times 20$  years = 6.58%. While these  
448 estimates are much lower, many host trees of sap feeders and defoliators are very common, and  
449 this mortality could very well be inflating the perceived background mortality rates of these host  
450 trees measured in [12].

451

#### 452 Management costs

453 As a final layer that allowed us to move from mortality estimates to cost estimates, we estimated  
454 the cost of removing and replacing dead trees. We used this cost because we believe it to be the  
455 minimum management response required, and because the extent and variability of preventive  
456 behaviour would be much harder to estimate. However, we note that this cost does not account  
457 for additional preventive cutting or any non-cutting management such as spraying or soil  
458 drenching with pesticides. We assumed that cutting was a one-time 100% effective treatment  
459 against IAFIs, or in other words, that newly planted trees were of different species and thus not  
460 susceptible to the same IAFI species that killed the previous trees. We assumed a 2% discount  
461 rate for future damages [1] and also that infestations were independent, or in other words that  
462 invasion by one IAFI did not interfere with invasion by another. This is likely a fair assumption, as  
463 there is minimal host sharing across IAFIs, and IAFI species each infest only a small proportion of  
464 hosts at a given time interval, so there is minimal potential for species interactions [30]. We  
465 assumed the same per-tree cost estimates for cutting and replacing dead trees as in [1], where  
466 the cost of cutting increases nonlinearly with size class. If we assume that street trees are always  
467 under the jurisdiction of local governments, the cost of removal and replacement of each tree is  
468 US\$450 for small trees, US\$600 for medium trees, and US\$1200 for large trees (these costs  
469 jump to an estimated US\$600, US\$800, and US\$1500 for homeowners). We reported all costs  
470 incurred from 2020 to 2050 in 2019 US dollars based on a 2% discount rate relative to these  
471 baseline costs. Since these baseline per-tree management costs came from a 2011 publication,  
472 we converted them to 2019 dollars via the consumer price index, which amounted to an inflation  
473 of 13.65% (World Bank, <https://data.worldbank.org>), though we note that the present-day costs of  
474 per-tree removal may have declined with advances in technology.

475

#### 476 Model synthesis

477 Once all subcomponent models had been parameterized, we synthesized the street tree  
478 estimates, IAFI spread estimates, host mortality estimates, and removal costs to produce overall  
479 cost estimates (Fig. S1). We summed the damages from 2020 to 2050 to obtain a total

480 discounted cost for this 30-year window. We then obtained annualized costs by calculating an  
481 annuity over the 30-year time horizon using the following equation:

$$482 \quad \text{Annualized damage} = D \frac{\sum_{time=min}^{max} Cost_{time}}{(1-(1+D)^{min-max})} \quad (4)$$

483 Where D is the discount rate (2%). Using these forecasts, we extended the concept of  
484 cost-curves from [1], which were based on frequencies of occurrences of low and intermediate  
485 damaging IAFI, and explicit economic estimates of three 'poster pests'. To parameterize the cost-  
486 curves in this manuscript, rather than just 3 poster pests, we estimated street tree costs for all 57  
487 intermediate-impact IAFIs across the 3 major insect feeding guilds, in addition to frequencies of  
488 low-impact species (Table S4.1). The summed area under each guild-specific curve can be  
489 interpreted as the estimate of the total annualized cost of all IAFIs in the US to street trees. Since  
490 our curves were missing only low-impact species, the total cost estimated with these approaches  
491 is not appreciably different from a simple sum of the costs of the non-missing (57 intermediate)  
492 species reported in text, but we included these analyses to allow for the prediction of the costs of  
493 novel invaders from each guild (Appendix S4).

494 We assessed parameter uncertainty in proportional host mortality by sampling from our  
495 posterior beta mortality distribution. We also used sensitivity analysis to explore the effect of  
496 different mortality debt scenarios, including 1) our most likely scenario, 2) setting all guilds to 10,  
497 50, or 100-year debts, and 3) varying each guild separately while holding the other two guilds at  
498 their most likely scenario. While our host distribution models were based on standard modelling  
499 approaches (e.g. GAM), our Bayesian formulations underlying the mortality estimates were novel  
500 and needed to be tested theoretically, to ensure that parameters were identifiable, and  
501 reproduced the correct behavior. See Appendix S4 for details of our theoretic analyses.

#### 502 Potential impacts to non-street trees

503 To provide a rough estimate of non-street tree impacts, we built a model for whole-community  
504 trees (i.e., street + non-street trees) from the dataset of 56 communities where genus-level  
505 estimates were reported, subtracted predicted street trees from this whole community estimate,  
506 and apportioned the remaining trees into residential and non-residential trees based on their  
507 average fractions across all sites where land type breakdowns were provided (32 municipalities).  
508 Given the relatively limited data, we caution against overinterpretation of these results.

#### 509 **Acknowledgments**

510  
511  
512 EJH would like to thank her PhD supervisory committee members T. Jonathan Davies and  
513 Patrick M. A. James for their invaluable comments, as well as the thoughtful comments and  
514 questions from thesis external examiner Dominique Gravel and colleague Andrew Liebhold. EJH  
515 also acknowledges the continual support and feedback from lab members Dat Nguyen, Abbie  
516 Gail Jones, Charlotte Steeves, Shriram Varadarajan, and Lidia Della Venezia. This work was  
517 supported by a NSERC CGS-D awarded to EJH. This research was funded, in part, through Cost  
518 Share Agreements 17-CS-11330110-025, 18-CS-11330110-026, and 19-CS-11330110-027,  
519 between the USDA Forest Service and North Carolina State University.

#### 520 **References**

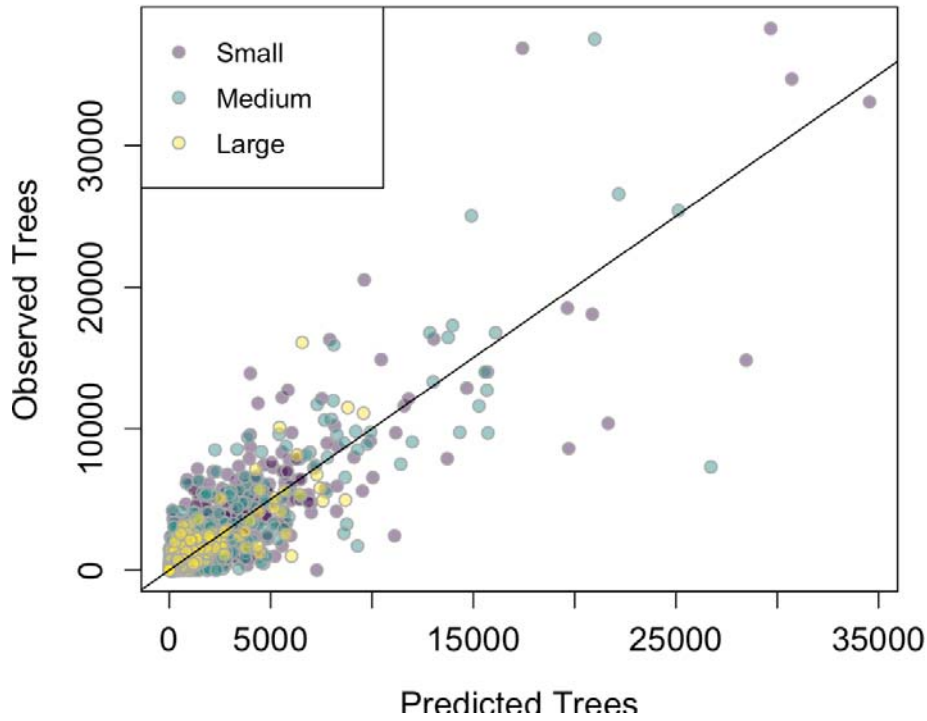
- 521 1. Aukema, J. E., Leung, B., Kovacs, K., Chivers, C., Britton, K. O., Englin, J., ... *et al.*  
522 (2011). Economic impacts of non-native forest insects in the continental United States.  
523 *PLoS One*, 6(9).
- 524 2. Kovacs, K. F., Haight, R. G., McCullough, D. G., Mercader, R. J., Siegert, N. W., &  
525 Liebhold, A. M. (2010). Cost of potential emerald ash borer damage in US communities,  
526 2009–2019. *Ecological Economics*, 69(3), 569-578.

- 530 3. Fahrner, S. J., Abrahamson, M., Venette, R. C., & Aukema, B. H. (2017). Strategic  
531 removal of host trees in isolated, satellite infestations of emerald ash borer can reduce  
532 population growth. *Urban Forestry & Urban Greening*, 24, 184-194.
- 533 4. Norton, B. A., Coutts, A. M., Livesley, S. J., Harris, R. J., Hunter, A. M., & Williams, N. S.  
534 (2015). Planning for cooler cities: A framework to prioritise green infrastructure to mitigate  
535 high temperatures in urban landscapes. *Landscape and Urban Planning*, 134, 127-138.
- 536 5. Van den Berg, A. E., Maas, J., Verheij, R. A., & Groenewegen, P. P. (2010). Green space  
537 as a buffer between stressful life events and health. *Social science & medicine*, 70(8),  
538 1203-1210.
- 539 6. Roy, S., Byrne, J., & Pickering, C. (2012). A systematic quantitative review of urban tree  
540 benefits, costs, and assessment methods across cities in different climatic zones. *Urban  
541 Forestry & Urban Greening*, 11(4), 351-363.
- 542 7. Hulme, P. E. (2009). Trade, transport and trouble: managing invasive species pathways  
543 in an era of globalization. *Journal of Applied Ecology*, 46(1), 10-18.
- 544 8. Hudgins, E. J., Liebhold, A. M., & Leung, B. (2017). Predicting the spread of all invasive  
545 forest pests in the United States. *Ecology letters*, 20(4), 426-435.
- 546 9. Hudgins, E. J., Liebhold, A. M., & Leung, B. (2020). Comparing generalized and  
547 customized spread models for nonnative forest pests. *Ecological Applications*, 30(1),  
548 e01988.
- 549 10. IPPC (International Plant Protection Convention). 2002. International standards for  
550 phytosanitary measures. Rome, Italy: FAO.  
551 [www.fao.org/docrep/009/a0450e/a0450e00.htm](http://www.fao.org/docrep/009/a0450e/a0450e00.htm). Viewed 12 May 2020.
- 552 11. Leung, B., Springborn, M. R., Turner, J. A., & Brockerhoff, E. G. (2014). Pathway-level  
553 risk analysis: the net present value of an invasive species policy in the US. *Frontiers in  
554 Ecology and the Environment*, 12(5), 273-279.  
555
- 556 12. Hilbert, D. R., Roman, L. A., Koeser, A. K., Vogt, J., & van Doorn, N. S. (2019). Urban  
557 tree mortality: a literature review. *Arboriculture & Urban Forestry*: 45 (5): 167-200., 45(5),  
558 167-200.
- 559 13. Paap, T., Burgess, T. I., & Wingfield, M. J. (2017). Urban trees: bridge-heads for forest  
560 pest invasions and sentinels for early detection. *Biological Invasions*, 19(12), 3515-3526.  
561
- 562 14. Kovacs, K., Václavík, T., Haight, R. G., Pang, A., Cunniffe, N. J., Gilligan, C. A., &  
563 Meentemeyer, R. K. (2011). Predicting the economic costs and property value losses  
564 attributed to sudden oak death damage in California (2010–2020). *Journal of  
565 Environmental Management*, 92(4), 1292-1302.  
566
- 567 15. Koch, F. H., Ambrose, M. J., Yemshanov, D., Wiseman, P. E., & Cowett, F. D. (2018).  
568 Modeling urban distributions of host trees for invasive forest insects in the eastern and  
569 central USA: A three-step approach using field inventory data. *Forest Ecology and  
570 Management*, 417, 222-236.
- 571 16. Potter, K. M., Escanferla, M. E., Jetton, R. M., & Man, G. (2019). Important insect and  
572 disease threats to United States tree species and geographic patterns of their potential  
573 impacts. *Forests*, 10(4), 304.

- 574 17. McGeoch, M. A., Genovesi, P., Bellingham, P. J., Costello, M. J., McGrannachan, C., &  
575 Sheppard, A. (2016). Prioritizing species, pathways, and sites to achieve conservation  
576 targets for biological invasion. *Biological Invasions*, 18(2), 299-314.
- 577 18. Sardain, A., Sardain, E., & Leung, B. (2019). Global forecasts of shipping traffic and  
578 biological invasions to 2050. *Nature Sustainability*, 2(4), 274-282.
- 579  
580 19. Haack, R. A., Hérard, F., Sun, J., & Turgeon, J. J. (2010). Managing invasive populations  
581 of Asian longhorned beetle and citrus longhorned beetle: a worldwide  
582 perspective. *Annual review of entomology*, 55.
- 583 20. Lovett, G. M., Weiss, M., Liebhold, A. M., Holmes, T. P., Leung, B., Lambert, K. F., ... &  
584 Weldy, T. (2016). Nonnative forest insects and pathogens in the United States: Impacts  
585 and policy options. *Ecological Applications*, 26(5), 1437-1455.
- 586  
587 21. Knight, K. S., Brown, J. P., & Long, R. P. (2013). Factors affecting the survival of ash  
588 (*Fraxinus* spp.) trees infested by emerald ash borer (*Agrilus planipennis*). *Biological*  
589 *Invasions*, 15(2), 371-383.
- 590 22. Fei, S., Morin, R. S., Oswalt, C. M., & Liebhold, A. M. (2019). Biomass losses resulting  
591 from insect and disease invasions in US forests. *Proceedings of the National Academy of*  
592 *Sciences*, 116(35), 17371-17376.
- 593 23. Kinloch Jr, B. B. (2003). White pine blister rust in North America: past and  
594 prognosis. *Phytopathology*, 93(8), 1044-1047.
- 595  
596 24. Rizzo, D. M., & Garbelotto, M. (2003). Sudden oak death: endangering California and  
597 Oregon forest ecosystems. *Frontiers in Ecology and the Environment*, 1(4), 197-204.
- 598  
599 25. Coleman, T. W., Poloni, A. L., Chen, Y., Thu, P. Q., Li, Q., Sun, J., ... *et al.* (2019).  
600 Hardwood injury and mortality associated with two shot hole borers, *Euwallacea* spp., in  
601 the invaded region of southern California, USA, and the native region of Southeast  
602 Asia. *Annals of Forest Science*, 76(3), 1-18.
- 603  
604 26. Coutts, S. R., Helmstedt, K. J., & Bennett, J. R. (2018). Invasion lags: The stories we tell  
605 ourselves and our inability to infer process from pattern. *Diversity and*  
606 *Distributions*, 24(2), 244-251.
- 607  
608 27. Hijmans, R. J., Phillips, S., Leathwick, J., Elith, J., & Hijmans, M. R. J. (2017). Package  
609 'dismo'. *Circles*, 9(1), 1-68.
- 610 28. Fick, S. E., & Hijmans, R. J. (2017). WorldClim 2: new 1-km spatial resolution climate  
611 surfaces for global land areas. *International Journal of Climatology*, 37(12), 4302-4315.
- 612 29. Homer, C.G., Dewitz, J.A., Yang, L., Jin, S., Danielson, P., Xian, G., ... *et al.* (2015.)  
613 Completion of the 2011 National Land Cover Database for the conterminous United  
614 States – representing a decade of land cover change information. *Photogrammetric*  
615 *Engineering and Remote Sensing*, 81, 345–354.
- 616 30. Amodio, S., Aria, M., & D'Ambrosio, A. (2014). On concavity in nonlinear and  
617 nonparametric regression models. *Statistica*, 74(1), 85-98.
- 618 31. Lambert, D. (1992). Zero-inflated Poisson regression, with an application to defects in  
619 manufacturing. *Technometrics*, 34(1), 1-14.

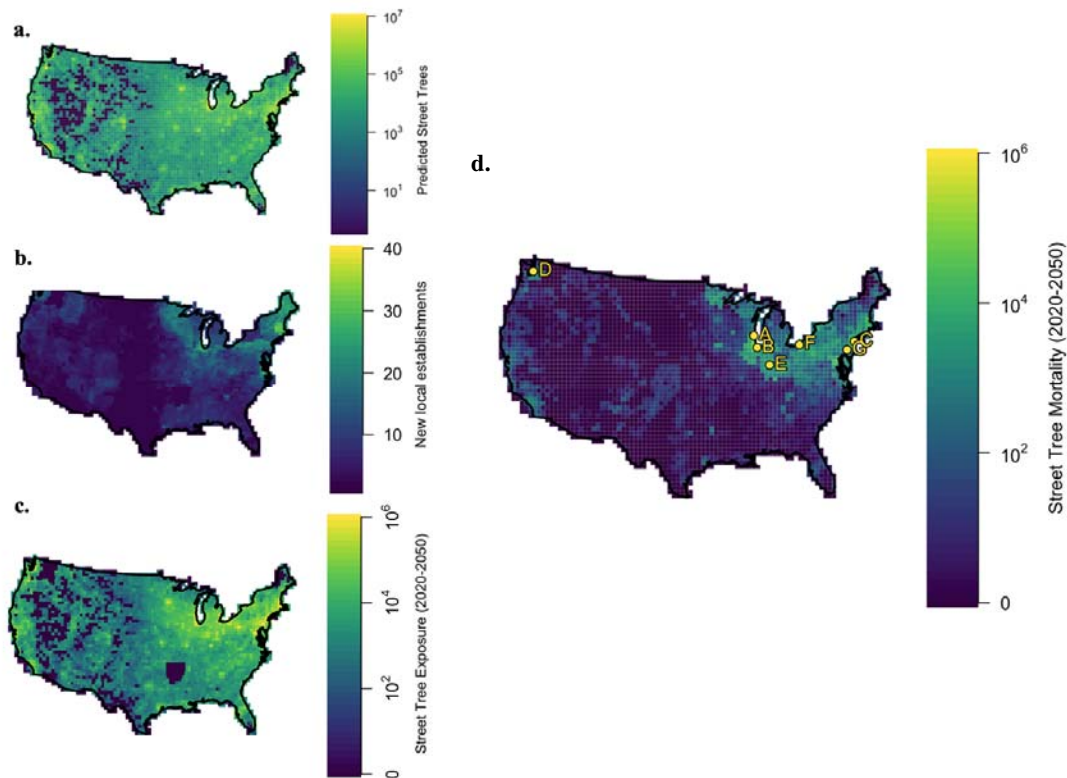
- 620 32. Wood, S. (2012). *mgcv: Mixed GAM Computation Vehicle with GCV/AIC/REML*  
621 *smoothness estimation*. R package.
- 622 33. Elith, J., Leathwick, J. R., & Hastie, T. (2008). A working guide to boosted regression  
623 trees. *Journal of Animal Ecology*, 77(4), 802-813.
- 624 34. Aukema, J. E., McCullough, D. G., Von Holle, B., Liebhold, A. M., Britton, K., & Frankel,  
625 S. J. (2010). Historical accumulation of nonindigenous forest pests in the continental  
626 United States. *BioScience*, 60(11), 886-897.
- 627 35. Carpenter, B., Gelman, A., Hoffman, M. D., Lee, D., Goodrich, B., Betancourt, M., ... *et al.*  
628 (2017). Stan: A probabilistic programming language. *Journal of Statistical*  
629 *Software*, 76(1).
- 630 36. Pugh, S.A. (2010). *Michigan's forest resources, 2008*. Research Note NRS-50. Newtown  
631 Square, PA: U.S. Forest Service, Northern Research Station. 4 pp.
- 632
- 633 37. Hochberg, M.E., & Weis, A.E. (2001). Ecology: bagging the lag. *Nature* 409, 992–93.
- 634 38. Liebhold, A.M., & Tobin, P.C. (2008). Population ecology of insect invasions and their  
635 management. *Annual Review of Entomology*, 53, 387–408.

636 **Figures and Tables**  
637



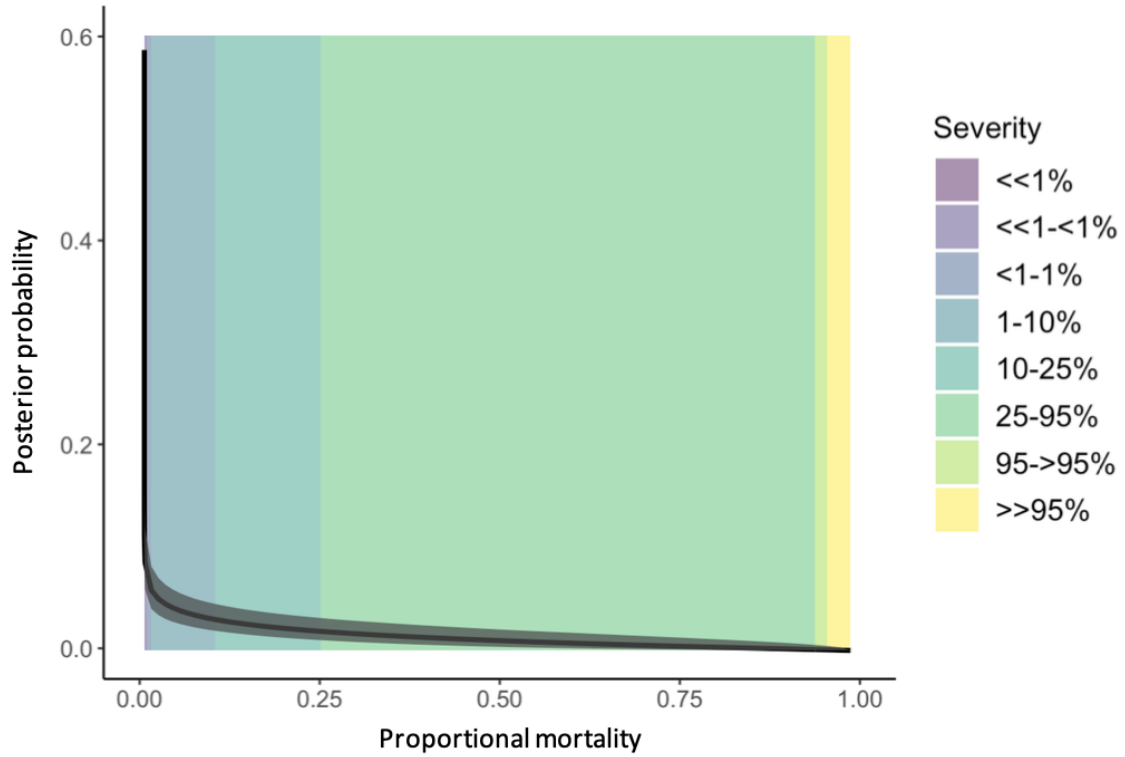
638  
639  
640

**Figure 1.** Fit of the genus-specific host tree models across all genera and size classes.



641 **Figure 2.** Model outputs for the first three subcomponent models, including **a.** predicted street  
642 tree abundance, **b.** predicted newly invaded sites of existing IAFIs, **c.** predicted street tree  
643 exposure levels (number of focal host tree + IAFI interactions) from 2020 to 2050, and finally **d.**  
644 Predicted total tree mortality from 2020 to 2050 in the most likely mortality debt scenario across  
645 space. The top seven most impacted cities or groups of nearby cities are shown in terms of total  
646 tree mortality 2020 to 2050 (A = Milwaukee, WI; B = Chicago/Aurora/Naperville/Arlington Heights,  
647 IL; C = New York, NY; D = Seattle, WA; E = Indianapolis, IN; F = Cleveland, OH; G =  
648 Philadelphia, PA).  
649

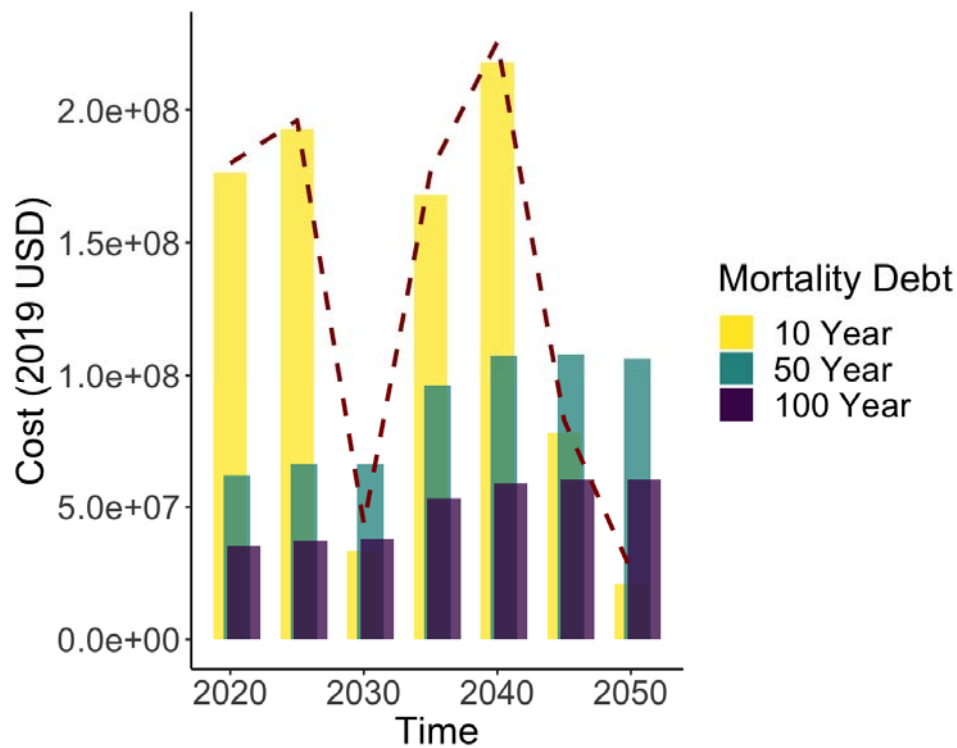




650

651

652 **Figure 3.** Posterior distribution for the beta model of host mortality due to IAFIs within each  
653 severity category. 95% Bayesian credible intervals are shown in grey, and the posterior median is  
654 shown in black. Colored bins represent severity categories extended from [14].



655  
656  
657  
658  
659  
660

**Figure 4.** Depiction of the influence of mortality debt on temporal cost patterns. Predicted costs 2020 to 2050 for the 10 year (yellow), 50 year (teal), and 100 year (purple) mortality debt scenarios with a 10 year initial invasion lag. The most likely scenario predictions are shown as a dashed red line. Costs are presented in 5-year increments in accordance with the timestep length within our spread model.

661 **Table 1.** Predicted annualized cost (in 2019 US dollars) and tree mortality across invasion  
 662 scenarios from 2020 to 2050 across all 57 IAFI species. “Most likely” indicates the scenario with  
 663 expert-elicited mortality debt durations by feeding guild, “Vary” scenarios hold all guilds but the  
 664 focal guild constant at their most likely scenario, and “All” fix all three guilds at a given mortality  
 665 debt duration. Mean mortality for most likely scenario = 2.3%, 1.38M trees, US\$ 30M annualized  
 666 (US\$ 679M over the next 30 years).  
 667

Mortality Debt Scenario	Annualized Cost (US\$ millions)		Tree Mortality (Millions)		Percent Mortality	
	lower 95% CI	upper 95% CI	lower 95% CI	upper 95% CI	lower 95% CI	upper 95% CI
Most likely	28.5	33.2	1.29	1.54	2.1%	2.5%
Vary Borers	10.1	32.1	0.45	1.45	0.7%	2.4%
Vary Defoliators	28.1	32.6	1.28	1.48	2.1%	2.4%
Vary Sap-feeders	28.5	32.5	1.30	1.47	2.1%	2.4%
All 10	27.8	30.4	1.27	1.39	2.1%	2.3%
All 50	18.5	22.3	0.84	1.00	1.4%	1.7%
All 100	9.77	13.5	0.44	0.60	0.7%	1.0%

668